Research Letter DOI: 10.15541/jim20230278

Self-polarization Achieved by Compositionally Gradient Doping in $BiFeO_3$ Thin Films

DAI Le[1], LIU Yang[1], GAO Xuan[1], WANG Shuhao[1], SONG Yating[1], TANG Mingmeng[1], DMITRY V Karpinsky[2], LIU Lisha[1], WANG Yaojin[1]

(1. School of Materials Science and Engineering, Nanjing University of Science and Technology, Nanjing 210094, China; Scientific and Practical Centre for Materials Research, National Academy of Sciences of Belarus, Minsk 220072, Belarus)

Abstract: $BiFeO_3$ is a highly promising lead-free ferroelectric material, surpassing most conventional ferroelectric materials in terms of the polarization and Curie temperature, offering a pathway for potential applications at elevated temperatures. Nevertheless, challenges arise due to strong clamping effect of substrate, large coercive fields, and high leakage currents, causing $BiFeO_3$ films difficult to be polarized. The implementation of self-polarization presents a viable solution. Herein, we prepared $BiFeO_3$, up-graded films (which transition from $BiFeO_3$ to $Bi_{0.80}Ca_{0.20}FeO_{2.90}$ from the substrate to the film surface), and down-graded films (which transition from $Bi_{0.80}Ca_{0.20}FeO_{2.90}$ to $BiFeO_3$ from the substrate to the film surface) using the Sol-Gel method on Pt(111)/Ti/SiO_2/Si substrates. After directional distribution of defects within the film being carefully modulated, the $BiFeO_3$ films are self-polarization when induced by build-in electric field. Piezoresponse force microscopy show that the up-graded and down-graded self-polarization behavior can be modulated by gradient direction of Ca in $BiFeO_3$ thin films. Moreover, diode-like current-voltage signature verifies the composition gradient-induced self-polarization. The X-ray photoelectron spectroscopy results indicate that the polarization orientation mechanism may arise from the internal electric field attributed to the gradient distribution of oxygen vacancy. This work provides a new strategy to achieve self-polarization in ferroelectric thin films, as well potential novel application in improving the performance of photovoltaic or photosensitive devices as assisted by internal field *via* self-aligned ferroelectric polarization.

Key words: self-polarization; gradient doping; bismuth ferrite film; Sol-Gel method

Spontaneous polarizations as regulated by different domains in as-prepared ferroelectric thin films normally shows random orientation and thus a zero net polarization. Thus, an external electric field applied to achieve polarization alignment is normally required for ferroelectric films to ensure its applications. Currently, polarized ferroelectric films with significant macroscopic piezoelectricity have widespread application in various fields, including micro-pumps, actuators, mass sensors, and micromachined ultrasonic transducers used in medical and sonar applications[1-2]. Whereas those providing high internal field due to aligned polarization but inferior piezoelectricity facilitate novel application in ferroelectric photocatalysis field, for instance, inspiring separation of charge carriers in photovoltaic devices as assisted by ferroelectric films with polarization alignment[3-5]. However, ferroelectric film tends to depolarize easily after being poled by external field, and the regular polarization arrangement reverts to a chaotic arrangement, maintaining the regular arrangement only for a short time. Therefore, if ferroelectric polarization in thin films can spontaneously become aligned without any electrode and external electric field excitation, it will be a great outlet and application for the design of some ferroelectric heterostructures and devices[6-8]. This effect was called "self-polarization" [9].

The ferroelectric films self-polarization has been previously reported, for instance, films of $PbTiO_3$[10-11],

Received date: 2023-06-12; **Revised date:** 2023-08-07; **Published online:** 2023-10-07
Foundation item: National Natural Science Foundation of China (52102133); Natural Science Foundation of Jiangsu Province, China (BK20210354); Fundamental Research Funds for the Central Universities (30921011217); Young Elite Scientists Sponsorship Program by CAST (2021-2023QNRC001)
Biography: DAI Le (1998–), female, Master candidate. E-mail: DL_2323@163.com
戴 乐(1998–), 女, 硕士研究生. E-mail: DL_2323@163.com
Corresponding author: WANG Yaojin, professor. E-mail: yjwang@njust.edu.cn; LIU Lisha, professor. E-mail: lishaliu@njust.edu.cn
汪尧进, 教授. E-mail: yjwang@njust.edu.cn; 刘丽莎, 教授. E-mail: lishaliu@njust.edu.cn

$Pb(Zr,Ti)O_3$[12], $BaTiO_3$[13-14], $Bi_{0.5}Na_{0.5}TiO_3$[15-17] and $BiFeO_3$[18-19]. Currently, researches focus on single crystal or epitaxial thin films, in that internal built-in electric field which counteracts the strong depolarization field can be easily formed through defects regulation[20-21], interfacial electrode effect[22-23], intrinsic property of the interface[13], flexoelectric effect[18], or epitaxial strain effect[24]. Compared with epitaxial thin films, polycrystalline ferroelectric thin films have the advantages of simple preparation process, low cost and suitable for wide range of growth. Therefore, how to realize self-polarization behavior in polycrystalline ferroelectric thin films deserves further research, especially with layer-by-layer deposition method of Sol-Gel. With this strategy, Zhao *et al.*[15] prepared polycrystalline BNT films with recoverable self-polarization that excel in settings with strong electric fields and high temperatures, which shows a prosperous research direction in this filed.

Perovskite bismuth ferrite, $BiFeO_3$ (BFO), possesses a variety of notable and uncommon characteristics, including an exceptionally high Curie temperature ($T_C \approx 830$ ℃), a large remanent polarization ($P_r \approx 100$ μC/cm^2) and multiferroic properties at room temperature[25]. However, controlling the polarization of ferroelectrics through an applied electric field is a challenge due to the presence of large leakage current and coercive field, either by corona polarization or contact polarization[26]. In this work, we focus on the fabrication of gradient Ca-doped BFO polycrystalline thin films on Pt(111)/Ti/SiO_2/Si substrates. Piezoresponse force microscope (PFM) was used to characterize the polarization switching behaviors, phase hysteresis loops and amplitude butterfly curves of BFO-based films. The phase images acquired through PFM reveal the presence of self-polarization in gradient doped films. The change of the self-polarization could result in large variations of the functional properties of the as-grown BFO films, such as diode behavior and ferroelectric properties.

1 Experimental

The Ca-doped $BiFeO_3$ (*i.e.*, $Bi_{1-x}Ca_xFeO_{3-x/2}$, x=0, 0.05, 0.10, 0.15, 0.20) (BCFO), $BiFeO_3$/$Bi_{0.95}Ca_{0.05}FeO_{2.975}$/$Bi_{0.90}Ca_{0.10}FeO_{2.950}$/$Bi_{0.85}Ca_{0.15}FeO_{2.925}$/$Bi_{0.80}Ca_{0.20}FeO_{2.90}$, (up-graded) and $Bi_{0.80}Ca_{0.20}FeO_{2.90}$/$Bi_{0.85}Ca_{0.15}FeO_{2.925}$/$Bi_{0.90}Ca_{0.10}FeO_{2.950}$/$Bi_{0.95}Ca_{0.05}FeO_{2.975}$/$BiFeO_3$ (down-graded), were spin-coated on Pt(111)/Ti/SiO_2/Si substrates *via* a Sol-Gel method. Bismuth nitrate ($Bi(NO_3)_3 \cdot 5H_2O$, 99.99%), iron nitrate ($Fe(NO_3)_3 \cdot 9H_2O$, 99.99%) and calcium nitrate ($Ca(NO_3)_2 \cdot 4H_2O$, 98.5%) were dissolved in 2-methoxyethanol (2-MOE) and stirred for 4 h at room temperature to prepare a solution used for fabricating BCFO films. In addition, the bismuth element is excess by 10% to compensate for the loss. All above raw materials were purchased from Aladdin. Finally, we acquired the $Bi_{1-x}Ca_xFeO_{3-x/2}$ (x=0, 0.05, 0.10, 0.15, 0.20) precursor solutions and the final concentration of the solutions was 0.25 mol/L. The Sol-Gel procedure included spin coating at 600 r/min for 10 s and at 4000 r/min for 30 s, and then dried at 200 ℃ for 120 s, pyrolyzed at 400 ℃ for 300 s, and annealed at 550 ℃ for 300 s in air using rapid thermal annealing. The drying, pyrolysis and annealing processes were repeated three times for each concentration of BCFO sol.

The crystal structure and orientation of the BFO-based films were studied by XRD (Bruker D8 Advance). X-ray photoelectron spectrometer (XPS, Thermo ESCALAB 250xi) using Al Kα radiation (1486.6 eV). The cross-sectional morphology and the distribution of element of BFO-based films were investigated by SEM (ZEISS Merlin) and EDS (Bruker super-X). The surface morphology was characterized with atomic force microscopy (AFM) (Bruker Multimode 8). Local piezoelectric responses imaging was conducted using piezoresponse force microscope mode of the AFM. Leakage current was obtained using a source meter (Keithley 2400). Ferroelectric properties were determined at 10 kHz on a ferroelectric measurement system (Multiferroic. Radiant Technology, USA). The laser Doppler vibrometer (MSA-100-3D Micro System Analyzer, Polytec GmbH, Germany) was utilized to measure the mechanical displacement in response to an applied sinusoidal voltage.

2 Results and discussion

The designed structures of up-graded films, down-graded films and BFO thin films are shown in Fig. 1(a-c), respectively. For up-graded films, starting from the substrate, the Ca doping concentration increases with the increase of thickness, and the doping amount is 0, 0.05, 0.10, 0.15, 0.20, respectively. Down-graded films are the opposite. In case Ca^{2+} substitutes for Bi^{3+} in the BFO lattice, it will lead to the formation of oxygen vacancies. It gives rise to a single charged acceptor center Ca'_{Bi}, which compensates for the oxygen vacancies formed. The defect equation is shown in Equation (1).

$$2CaO + Bi_2O_3 \rightarrow 2Ca'_{Bi} + 4O_O + V_O^{\cdot\cdot} \quad (1)$$

From which it can be deduced that higher concentrations of Ca doping are expected to generate a greater number of oxygen vacancies. Therefore, for gradient doped films (either up-graded or down-graded films), there would be distribution of oxygen vacancies due to compositionally

gradient of Ca, as shown in Fig. 1(a, b). This phenomenon has the potential to induce the formation of internal electric fields, consequently influencing the system's behavior in contrast to that of undoped BFO films. On the other hand, the internal spontaneous polarization is different with the replacement of Bi by Ca as shown by the gradient design. As shown in Fig. 1(d, e), the intensity of spontaneous polarization may be reduced after doping[27]. Thus, the polarization in each layer should have monotonous increase/decrease, leading to self-polarization, which could be the cause of self-polarization.

Firstly, the structure and cross-section morphology of the prepared films were characterized. The XRD patterns of all samples measured at room temperature are shown in Fig. 2(a). The XRD result reveals that all films exhibit well-crystallized structures with no detectable impurities or additional phases, confirming the successful doping of Ca into the perovskite BFO lattice. These results also indicate the homogeneity of the precursor solution and the appropriateness of the annealing process.

Fig. 2(b, f) show the cross-sectional SEM images of the up-graded and down-graded films, respectively. The images reveal the formation of columnar crystals in both films, and the measured thickness of the thin films

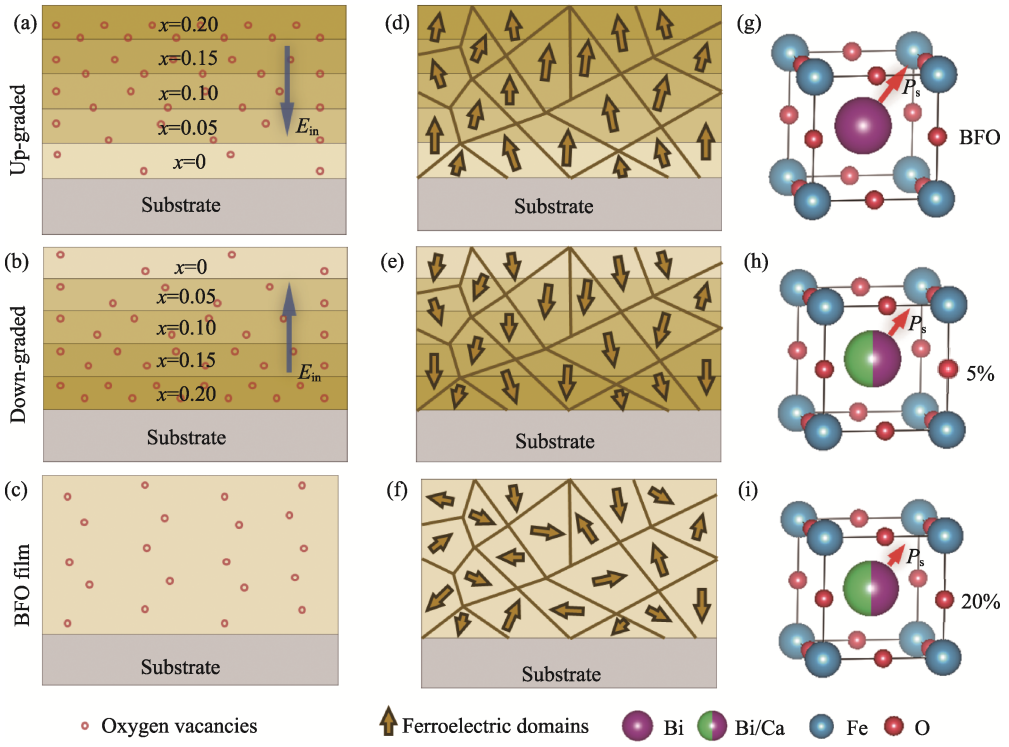

Fig. 1　(a-c) Schematic drawings of structures; Ferroelectric domains illustrating (d) up-graded film, (e) down-graded film and (f) BFO thin film; Schematic diagrams of crystal structures of BFO films (g) before and (h, i) after doping

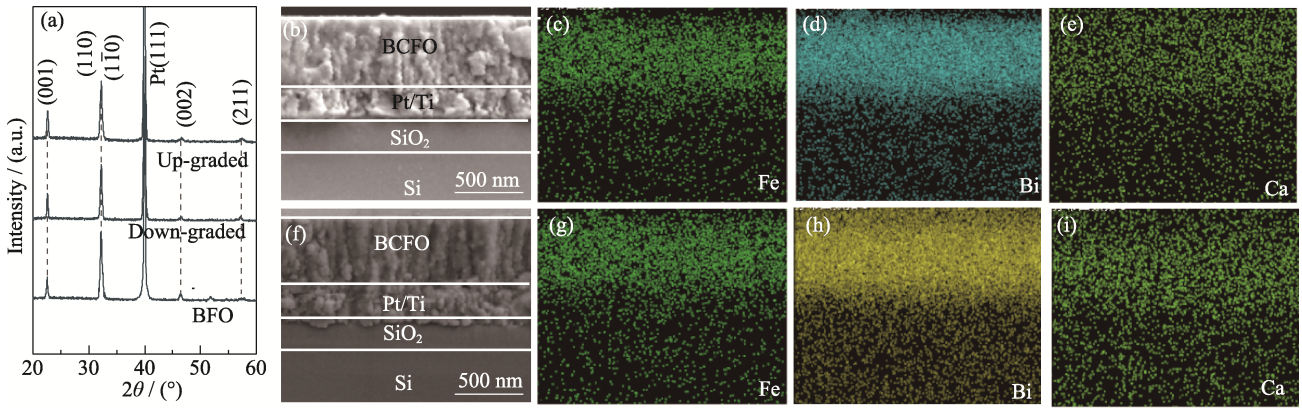

Fig. 2　Structures and cross section morphologies of thin films

(a) XRD patterns and SEM images of (b) up-graded films and (f) down-graded films. Bismuth, iron and calcium mappings of (c-e) up-graded BFO films and (g-i) down-graded BFO films

is approximately 500 nm. To examine the element distribution of the fabricated up-graded and down-graded films, the energy dispersive spectroscopy results are shown in Fig. 2(c-e) and Fig. 2(g-i), respectively. To some extent, it reflects a gradual change in the Ca and Bi ion concentration across the thickness of the compositionally graded films. However, the energy dispersive spectrum shows a limited resolution, that the elemental variation is slight.

The surface micrographs of all samples are shown in Fig. 3(a-c). It can be observed from the surface micrographs that all the films exhibit dense, uniform microstructures and small surface roughness. The R_q of up-graded films, down-graded films and BFO thin films are 1.26, 1.15 and 1.79 nm, respectively.

PFM was conducted to evaluate the local morphology and piezoelectric responses of all samples by applying an AC voltage of 3 V on 3 μm×3 μm area of the films surface through a conductive probe tip. Fig. 3(d-f) show the out-of-plane phase images of the studied samples. There are two distinguished colours in the phase images, the bright domains correspond to upward polarization, and dark domains result from the downward polarization. In the images, the up-graded films have upward self-polarization, while the down-graded films have downward self-polarization. In the case of BFO thin films and single doping concentration BCFO thin films (Fig. S1(b)), the phase images exhibit two distinct colors, suggesting the absence of self-polarization behavior. Fig. 3(g-i) show the phase hysteresis loop and the amplitude butterfly curve of all films. We observe the PFM hysteresis loop of up-graded films with a large positive coercive voltage (V–) of –5.484 V and a small negative coercive voltage (V+) of 0.281 V. The upward self- polarization phenomenon in the up-graded films is evident from the observed asymmetric switching characteristic, which is also corroborated by an amplitude butterfly curve. Similarly, for the down-graded films, PFM hysteresis loop exhibits

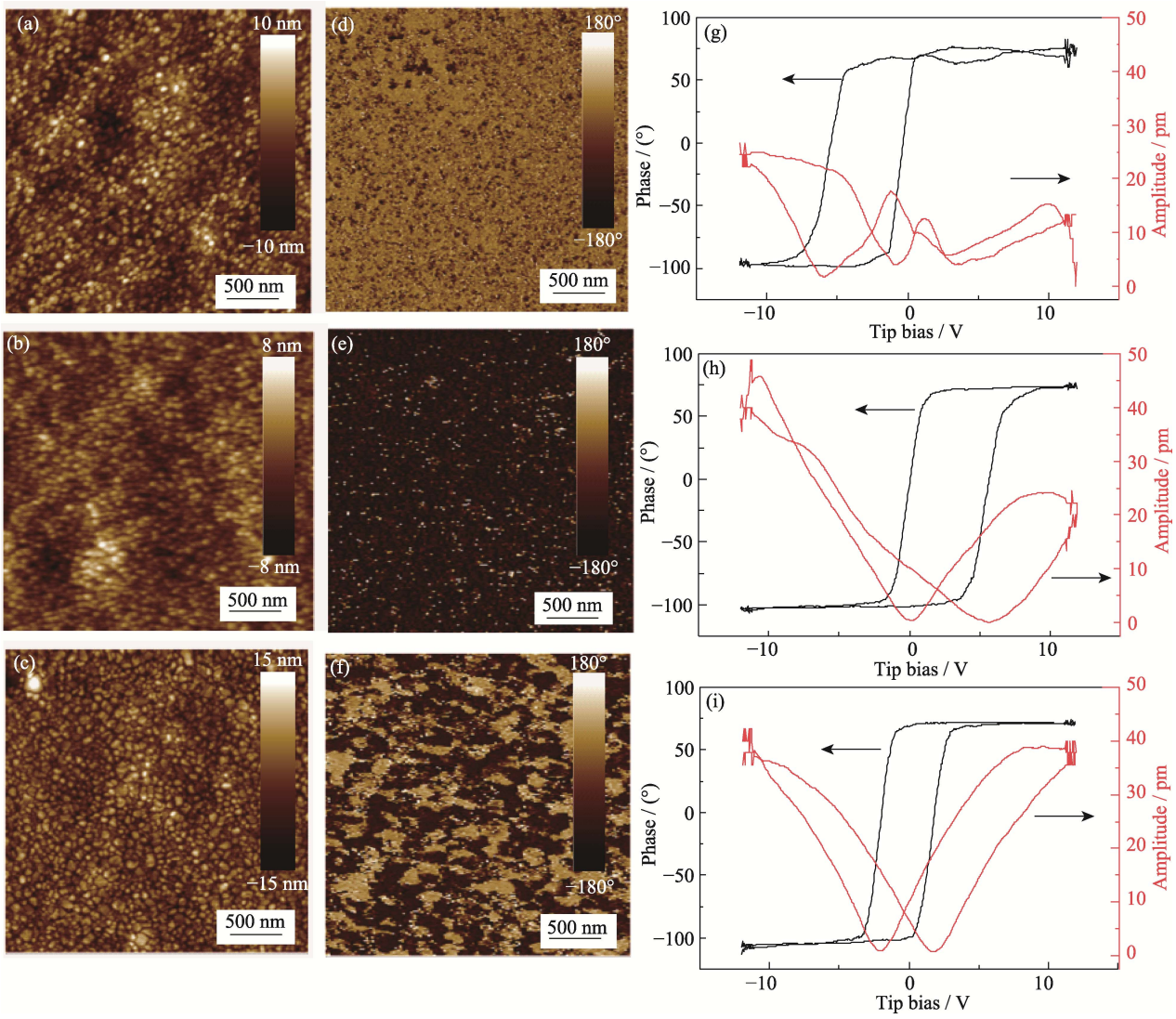

Fig. 3 Surface morphologies and domain structures of thin films

(a-c) AFM images, (d-f) out-of-plane PFM images, (g-i) accordingly asymmetric phase and amplitude loops *versus* tip bias voltage of (a, d, g) up-graded films, (b, e, h) down-graded films and (c, f, i) BFO films

a large positive coercive voltage (V+) of 5.672 V and a small negative coercive voltage (V–) of –0.047 V, providing evidence for the presence of the downward self-polarization phenomenon. In contrast, phase hysteresis loop and the amplitude butterfly curve of BFO thin films are symmetric, indicating that there is no self-polarization behavior for BFO films. PFM results indicate that the self-polarization direction of the films is contingent upon the direction of the Ca concentration gradient.

It is already known internal electric field can affect the transport properties such as diode behavior. We measured the current density-voltage (*J*-*V*) curves for the compositionally graded films and single doping concentration BCFO thin films. As shown in Fig. 4(a), the compositionally graded films demonstrate unidirectional conductive characteristic, where the up-graded films exhibit conductivity under positive bias and insulating behavior under negative bias, while the down-graded films show the opposite behavior. As shown in Fig. 4(b), under both positive and negative bias voltages, the BCFO thin films of single doping concentration exhibit remarkably comparable conductive behaviors. This discrepancy of conductive behaviors between gradient doped films and BCFO films of single doping concentration is attributed to internal electric field in gradient doped films, which caused the self-polarization effect. In addition, we can observe from Fig. 4(b), leakage currents decrease gradually with the addition of Ca, which is due to the reduction of grain size (Fig. S1(a)). At high voltage conditions, the leakage currents in gradient doped films are notably higher compared to BCFO thin films with a single doping concentration. This observation could be attributed to the increased presence of defects at the interface between different Ca doping concentrations in the films.

Fig. 5(a-c) display the ferroelectric polarization evolution as a function of the measured electric field for all prepared thin films. All measurements were conducted at room temperature with a frequency of 10 kHz. In general, well-defined *P*-*E* loops and larger breakdown strength can be measured for all thin films. It is noteworthy that, in contrast to the more square-like and sharper

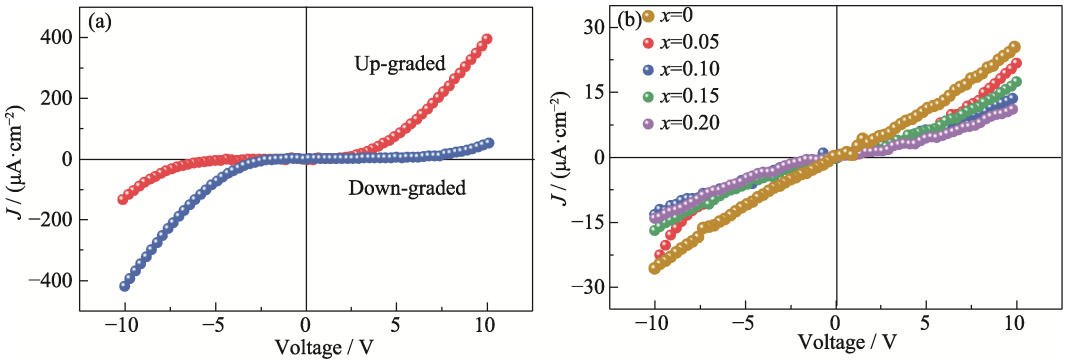

Fig. 4　*J*-*V* characteristics of thin films

(a) Up-graded BFO films and down-graded BFO films; (b) BCFO (x=0, 0.05, 0.10, 0.15, 0.20) films; Colorful figures are available on website

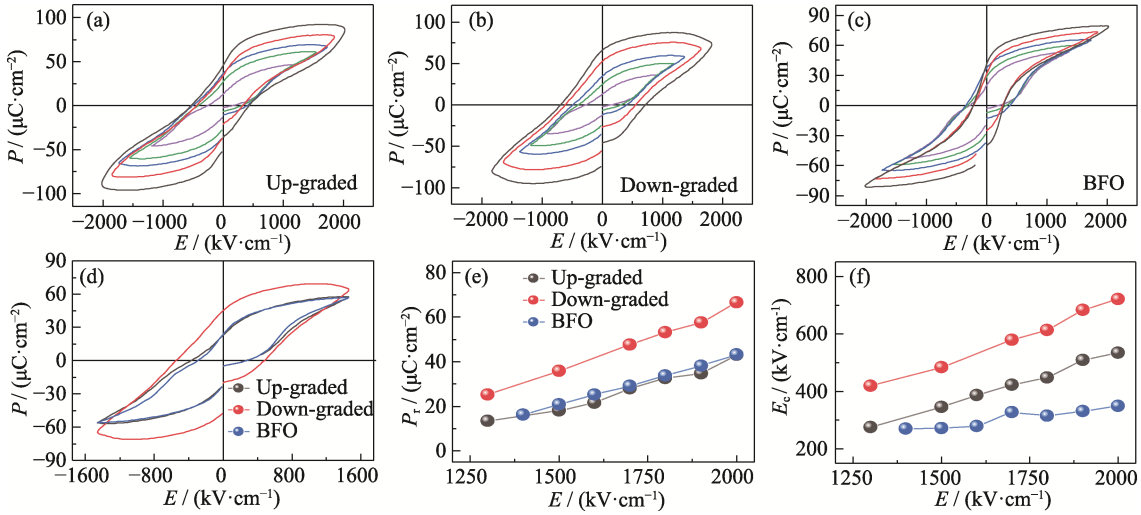

Fig. 5　Ferroelectric properties of BFO compositionally graded films

(a) Up-graded films; (b) Down-graded films; (c) BFO thin films; (d) Three kinds of films at the electric field intensity of 1500 kV/cm; (e) Remanent polarization, P_r and (f) coercive field, E_c changed with applied voltage; Colorful figures are available on website

P-E loops typically observed in BFO thin films, both up-graded and down-graded BFO films exhibit a significant leaky characteristic. This implies that there may be more defects at the interface between films with different Ca doping concentrations. These defects may respond to electric fields much easier at higher ranges, resulting in a transformation of the *P-E* loops to rounded-shape. Fig. 5(d) shows the ferroelectric switching behavior of all prepared thin films at the electric field of 1500 kV/cm. The remanent polarization, P_r, and the coercive field, E_c, are summarized and shown in Fig. 5(e, f), respectively. Obviously, the up-graded films exhibit higher P_r compared to the other films, while the down-graded films show similar P_r to that of pure BFO films. It is clear that P_r can reach 43.1, 66.6 and 43.1 μC/cm^2 at an electrical field of 2000 kV/cm for the up-graded films, down-graded films and BFO thin films, respectively. In addition, we can observe that E_c of the compositionally graded films is larger than that of undoped BFO films. Moreover, we measured the *P-E* loops of BFO films doped with a single concentration, as shown in Fig. S2. The lack of a monotonic change P_r in with increasing x indicates that self-polarization cannot be attributed to polarization variation within the gradient doped films.

As mentioned above, we consider that the cause of self-polarization is the directional arrangement of oxygen vacancies. In order to determine the elements, chemical shifts, oxidation state of the elements and oxygen vacancies of Ca-doped BFO samples, detailed XPS analyses were performed. The narrow scan XPS spectra of O1s, Fe2p and Ca2p for single doping concentration $Bi_{1-x}Ca_xFeO_3$ (x=0, 0.05, 0.10, 0.15 and 0.20) samples are shown in Fig. 6. The XPS spectra of O1s are illustrated in Fig. 6(a), which are de-convoluted into three peaks: the lower binding (LB) energy, medium binding (MB) energy and higher binding (HB) energy for samples. The LB energy, MB energy and HB energy of BCFO film were attributed to the oxygen present in the lattice, oxygen loss and absorbed oxygen on the surface, respectively. The percentages of the oxygen vacancy concentration, shown in Fig. 6(e), are found to be 22.8%, 22.4%, 25.9%, 27.9% and 37% for x=0, 0.05, 0.10, 0.15 and 0.20, respectively, as calculated by the ratio of MB/(LB+MB+HB)[28]. The obtained results align with the diagram depicted in Fig. 1(a, b), indicating that the monotonically increasing or decreasing oxygen vacancy concentration along the thickness direction could lead to the formation of an internal electric field.

Fig. 6(b) shows Fe2p XPS core spectra of BCFO samples. Two peaks between binding energies of 705–730 eV can be seen, which are attributed to the $Fe2p_{1/2}$ near 723.7 eV and the $Fe2p_{3/2}$ near 710.2 eV, respectively.

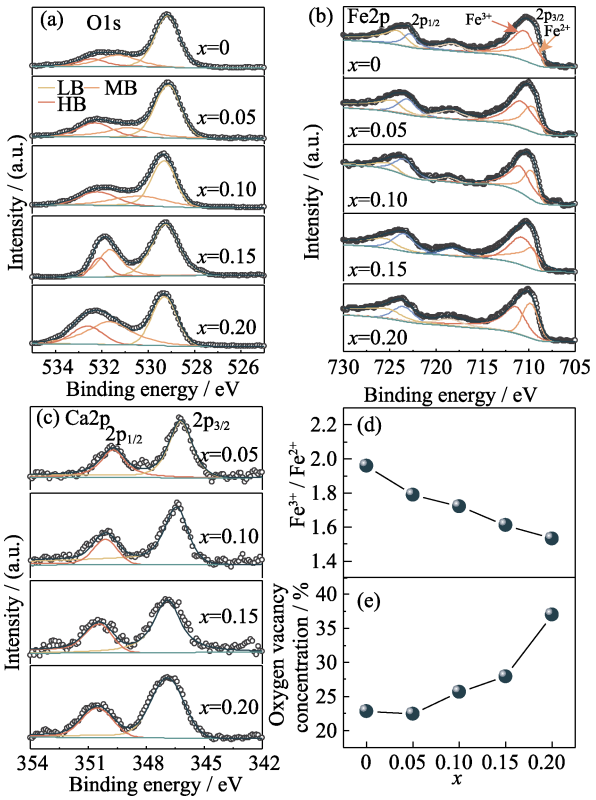

Fig. 6 Valence analysis of thin films

Narrow scan spectra of thin films: (a) O1s, (b) Fe2p, and (c) Ca2p of $Bi_{1-x}Ca_xFeO_3$ samples with x=0, 0.05, 0.10, 0.15 and 0.20; (d) Ratio of Fe^{3+}/Fe^{2+} and (e) percentage of the oxygen vacancy concentration of BFCO with the increase of x

Spin-orbit splitting energy is equal to 13.5 eV, which is comparable to the theoretical value of Fe2p (13.6 eV) for Fe_2O_3[29]. Moreover, it is commonly observed that Fe^{2+} and Fe^{3+} appear in BFO films. The ratio of Fe^{2+} to Fe^{3+} was calculated by deconvoluting and fitting the $Fe2p_{3/2}$ peaks. The Fe^{3+}/Fe^{2+} ratio decreases gradually from 1.96 : 1 for x=0 to 1.53 : 1 for x=0.20 shown in Fig. 6(e), which suggests that Ca doping concentration is positively correlated with the level of oxygen vacancy enhancement. Furthermore, despite the presence of a significant number of defects, the perovskite crystal structure remains intact. The Ca2p spectra deconvoluted into two wide peaks of $Ca2p_{3/2}$ ~346.2 eV and $Ca2p_{1/2}$ ~ 349.7 eV for x=0.05 are shown in Fig. 6(c), which are mainly ascribed to Ca–O bonds. It can be observed that slight shifting of Ca2p peaks towards the higher binding energy side with increasing doping concentration of Ca content in BFO samples. Based on the electronegativity values of Bi, Ca, and O elements, and by calculating the covalency/ionicity of Bi–O and Ca–O bonds, it is evident that the fraction of ionicity for the Ca–O bond (0.77) is considerably higher than that for the Bi–O bond (0.40). This observation suggests the bonding energy of the Ca–O bond within the oxygen octahedron exceeds that of the Bi–O bond[29]. That's why the peak Ca2p shifts towards the higher binding energy side.

Through the above results, we realize the self-polarization of BFO-based polycrystalline thin films by compositionally gradient doping of Ca. Several explanations for the self-polarization phenomenon have been put forth, including lattice misfit strain, intrinsic property of the interface and defects of regular arrangement and so on. In many epitaxial thin film systems, thermal strain or lattice misfit strain are important factors in determining the polarization behavior[24]. In polycrystalline films, the influence of these factors is generally not considered, suggesting that the strain gradient is unlikely to be the primary determinant of self-polarization in BFO films. Furthermore, the investigation of *P-E* loops for BCFO films with varying Ca doping concentrations (shown in Fig. S3) reveals a lack of a monotonic increase or decrease in polarization, indicating that it is not responsible for self-polarization.

An alternative explanation pertains to the presence of an internal electric field, which is typically observed at the interfaces between the films and the underlying electrodes. As it is widely recognized, the presence of a large depolarization field can lead to an unbalanced state, potentially rendering the self-polarization condition unstable. To counteract the strong depolarization field, the as-grown films must have an internal electric field built in. Studies have demonstrated that charged defects, such as oxygen vacancy, exhibit a preferential distribution, leading to the formation of an internal electric field. Then the domains within the ferroelectric film undergo polarization in response to the electric field generated by the defect dipoles[25]. Our study has revealed that the non-uniform distribution of oxygen vacancies in the film is a contributing factor to the generation of the internal electric field, which can be confirmed by Equation (1) and the XPS results shown in Fig. 6. And the presence of an internal electric field is supported by the asymmetric piezoresponse displayed in Fig. 3(g, h), as well as *J-V* characteristics depicted in Fig. 4(a). It can be inferred from the results that a downward internal electric field is formed in up-graded films, and an upward internal electric field is formed in down-graded films, which may cause their ferroelectric domains to be aligned, *i.e.*, self-polarization phenomenon, as shown in Fig. 1(d, e). Undoped BFO films lack a gradient distribution of oxygen vacancies, which precludes the existence of an internal electric field and the resultant phenomenon of regular ferroelectric domain arrangement.

However, perhaps due to these plenty of defects, the piezoelectric performance has been greatly degraded, resulting in a small value (~10 pm/V) shown in Fig. S4. In fact, the intrinsic piezoelectric constant of BFO film is small. Evgeniya *et al*.[30] reported on a self-poling effect in BFO thick films deposited by screen printing with a film thickness of 40 μm. However, despite the considerable thickness, the direct and converse piezoelectric coefficients were found to be only 18 pC/N and 25 pm/V, respectively. So, in the future, further investigations are worthwhile. Though d_{33} is intrinsically small for BFO, it still provides a strategy of great potential for applying in photovoltaic and photosensitive devices, which can be benefit from the internal electric field as provided by self-alignment of ferroelectric polarizations.

3 Conclusions

In conclusion, self-polarization characteristics were investigated by creating composition gradients in Ca-doped BFO thin films. PFM reveals the tunable nature of self-polarization behavior by the gradient direction of Ca in BFO thin films. The rectifying behavior of the *J-V* characteristic curves analyzed from the compositionally graded films is attributed to the arrangement of oxygen vacancies, which is supported by results of XPS analysis. Additionally, the self-polarization effect is supported by the results of converse piezoelectric measurements. This underlying mechanism responsible for the self-polarization phenomenon observed in polycrystalline BFO thin films, offers valuable insights for the fabrication of self-polarized polycrystalline thin films *via* Sol-Gel methods. Meanwhile, the findings provide a pathway for the development of diverse devices based on self-polarization effects.

Supporting materials

Supporting materials related to this article can be found at https://doi.org/10.15541/jim20230278.

References:

[1] JIN L, TANG X, SONG D, *et al*. Annealing temperature effects on (111)-oriented $BiFeO_3$ thin films deposited on Pt/Ti/SiO_2/Si by chemical solution deposition. *Journal of Materials Chemistry C*, 2015, **3(41):** 10742.

[2] XIAO M, LI S, LEI Z. Study of (111)-oriented PZT thin films prepared by a modified Sol-Gel method. *Journal of Materials Science: Materials in Electronics*, 2015, **26(6):** 4031.

[3] LI Z, ZHAO Y, LI W L, *et al*. Photovoltaic effect induced by self-polarization in $BiFeO_3$ films. *The Journal of Physical Chemistry C,* 2021, **125(17):** 9411.

[4] ZHANG Y, ZHENG H, WANG X, *et al*. Enhanced photovoltaic properties of gradient calcium-doped $BiFeO_3$ films. *Ceramics International*, 2020, **46(8):** 10083.

[5] LI Y, CUI X, TIAN M, *et al*. Stable photovoltaic output and optically tunable resistive switching in all-inorganic flexible ferroelectric thin film with self-polarization characteristic. *Acta Materialia*, 2021, **217(15):** 117173.

[6] HOU Y, HAN R, LIU Y, *et al*. Enhanced piezoelectric properties in $Li_xBi_{1-x}Nb_xFe_{1-x}O_3$ films contributed by low-symmetry phase and self-polarization. *Ceramics International*, 2019, **45(3):** 3723.

[7] LIU Y, DING L, DAI L, *et al.* All-ceramic flexible piezoelectric energy harvester. *Advanced Functional Materials*, 2022, **32(52):** 2209297.

[8] ZOU D, LIU S, ZHANG C, *et al.* Flexible and translucent PZT

films enhanced by the compositionally graded heterostructure for human body monitoring. *Nano Energy*, 2021, **85:** 105984.
[9] CHEN X, ZOU Y, YUAN G, *et al*. Temperature gradient introduced ferroelectric self-poling in $BiFeO_3$ ceramics. *Journal of the American Ceramic Society*, 2013, **96(12):** 3788.
[10] LICHTENSTEIGER C, WEYMANN C, FERNANDEZ-PENA S, *et al*. Built-in voltage in thin ferroelectric $PbTiO_3$ films: the effect of electrostatic boundary conditions. *New Journal of Physics*, 2016, **18(4):** 043030.
[11] FONG D, KOLPAK A, EASTMAN J, *et al*. Stabilization of monodomain polarization in ultrathin $PbTiO_3$ films. *Physical Review Letters*, 2006, **96(12):** 127601.
[12] PANTEL D, GOETZE S, HESSE D, *et al*. Room-temperature ferroelectric resistive switching in ultrathin $Pb(Zr_{0.2}Ti_{0.8})O_3$ films. A*CS Nano*, 2011, **5(7):** 6032.
[13] GUO R, SHEN L, WANG H, *et al*. Tailoring self-polarization of $BaTiO_3$ thin films by interface engineering and flexoelectric effect. *Advanced Materials Interfaces*, 2016, **3(23):** 1600737.
[14] HOU Y F, ZHANG T D, LI W L, *et al*. Self-polarization induced by lattice mismatch and defect dipole alignment in (001) $BaTiO_3/LaNiO_3$ polycrystalline film prepared by magnetron sputtering at low temperature. *RSC Advances*, 2015, **5(76):** 61821.
[15] ZHAO J, REN W, NIU G, *et al*. Recoverable self-polarization in lead-free bismuth sodium titanate piezoelectric thin films. *ACS Applied Materials & Interfaces*, 2017, **9(34):** 28716.
[16] ZHAO J, NIU G, REN W, *et al*. Self-polarization in epitaxial fully matched lead-free bismuth sodium titanate based ferroelectric thin films. *ACS Applied Materials & Interfaces*, 2018, **10(28):** 23945.
[17] ZHAO J, NIU G, REN W, *et al*. Polarization behavior of` lead-free $0.94(Bi_{0.5}Na_{0.5})TiO_3$-$0.06BaTiO_3$ thin films with enhanced ferroelectric properties. *Journal of the European Ceramic Society*, 2020, **40(12):** 3928.
[18] JEON B C, LEE D, LEE M H, *et al*. Flexoelectric effect in the reversal of self-polarization and associated changes in the electronic functional properties of $BiFeO_3$ thin films. *Advanced Materials*, 2013, **25(39):** 5643.
[19] HOU Y, LI W, ZHANG T, *et al*. Large piezoelectric response induced by the coexistence of low-symmetry and self-polarization in Li^+-Nb^{5+}-doped $BiFeO_3$ polycrystalline films. *The Journal of Physical Chemistry C*, 2016, **120(11):** 6246.
[20] CHISHOLM M F, LUO W, OXLEY M P, *et al*. Atomic-scale compensation phenomena at polar interfaces. *Physical Review Letters*, 2010, **105(19):** 197602.
[21] LIU C, LIU Y, ZHANG B, *et al*. Ferroelectric self-polarization controlled magnetic stratification and magnetic coupling in ultrathin $La_{0.67}Sr_{0.33}MnO_3$ films. *ACS Applied Materials & Interfaces*, 2021, **13(25):** 30137.
[22] CHU Y H, CRUZ M P, YANG C H, *et al*. Domain control in multiferroic bifeo$_3$ through substrate vicinality. *Advanced Materials*, 2007, **19(18):** 2662.
[23] BAEK S H, JANG H W, FOLKMAN C M, *et al*. Ferroelastic switching for nanoscale non-volatile magnetoelectric devices: 4. *Nature Materials*, 2010, **9(4):** 309.
[24] CHEN J, LUO Y, OU X, *et al*. Upward ferroelectric self-polarization induced by compressive epitaxial strain in (001) $BaTiO_3$ films. *Journal of Applied Physics*, 2013, **113(20):** 204105.
[25] WU J, FAN Z, XIAO D, *et al*. Multiferroic bismuth ferrite-based materials for multifunctional applications: ceramic bulks, thin films and nanostructures. *Progress in Materials Science*, 2016, **84:** 335.
[26] LI X, ZHANG L, LUO N, *et al*. Enhanced H_2S sensing performance of $BiFeO_3$ based MEMS gas sensor with corona poling. *Sensors and Actuators B: Chemical*, 2022, **358(1):** 131477.
[27] CAMPANINI M, ERNI R, YANG C, *et al*. Periodic giant polarization gradients in doped $BiFeO_3$ thin films. *Nano Letters*, 2018, **18(2):** 717.
[28] CHAUHAN S, KUMAR M, CHHOKER S, *et al*. Substitution driven structural and magnetic transformation in Ca-doped $BiFeO_3$ nanoparticles. *RSC Advances*, 2016, **6(49):** 43080.
[29] JIN L, TANG X, WEI R, *et al*. $BiFeO_3$(00l)/$LaNiO_3$/Si thin films with enhanced polarization: an all-solution approach. *RSC Advances*, 2016, **6(82):** 78629.
[30] KHOMYAKOVA E, SADL M, URSIC H, *et al*. Self-poling of $BiFeO_3$ thick films. *ACS Applied Materials & Interfaces*, 2016, **8(30):** 19626.

浓度梯度掺杂实现 $BiFeO_3$ 薄膜自极化

戴 乐[1], 刘 洋[1], 高 轩[1], 王书豪[1], 宋雅婷[1],
唐明猛[1], DMITRY V Karpinsky[2], 刘丽莎[1], 汪尧进[1]

(1. 南京理工大学 材料科学与工程学院, 南京 210094; 2. 白俄罗斯国家科学院 材料科学与应用研究中心, 明斯克 220072, 白俄罗斯)

摘 要: $BiFeO_3$ 是一种非常有前途的无铅铁电材料, 与大多数传统铁电材料相比, 它具有更大的极化和更高的居里温度, 为高温应用提供了可能。受到衬底强烈的夹持效应、较大的矫顽场和漏电流的影响, $BiFeO_3$ 薄膜难以被极化。自极化是解决这一问题的可行方法。本研究采用溶胶-凝胶法在 Pt(111)/Ti/SiO_2/Si 衬底上生长了 $BiFeO_3$ 薄膜, 向上梯度薄膜(从衬底 $BiFeO_3$ 过渡到薄膜表面 $Bi_{0.80}Ca_{0.20}FeO_{2.90}$)以及向下梯度薄膜(从衬底 $Bi_{0.80}Ca_{0.20}FeO_{2.90}$ 过渡到薄膜表面 $BiFeO_3$)。通过细致地调控薄膜内部缺陷的定向分布形成内置电场，从而导致薄膜具有自极化特性。压电力显微镜结果表明：在 $BiFeO_3$ 薄膜中, Ca 的梯度方向可以调控自极化的方向。此外, 类似二极管的单向导通特性验证了薄膜的自极化是由 Ca 的浓度梯度掺杂导致。X 射线光电子能谱结果表明, 氧空位的梯度分布导致的内置电场可能是造成自极化现象的原因。本研究为实现铁电薄膜的自极化提供了一种新的策略, 并在以自极化的内置电场为驱动, 提高光伏或光敏器件性能方面具有潜在的应用前景。

关 键 词: 自极化; 梯度掺杂; 铁酸铋薄膜; 溶胶-凝胶法

中图分类号: TB383 **文献标志码:** A **文章编号:** 1000-324X(2024)01-0099-08

Supporting materials:

Self-polarization Achieved by Compositionally Gradient Doping in $BiFeO_3$ Thin Films

DAI Le[1], LIU Yang[1], GAO Xuan[1], WANG Shuhao[1], SONG Yating[1], TANG Mingmeng[1], DMITRY V Karpinsky[2], LIU Lisha[1], WANG Yaojin[1]

(1. School of Materials Science and Engineering, Nanjing University of Science and Technology, Nanjing 210094, China; Scientific and Practical Centre for Materials Research, National Academy of Sciences of Belarus, Minsk 220072, Belarus)

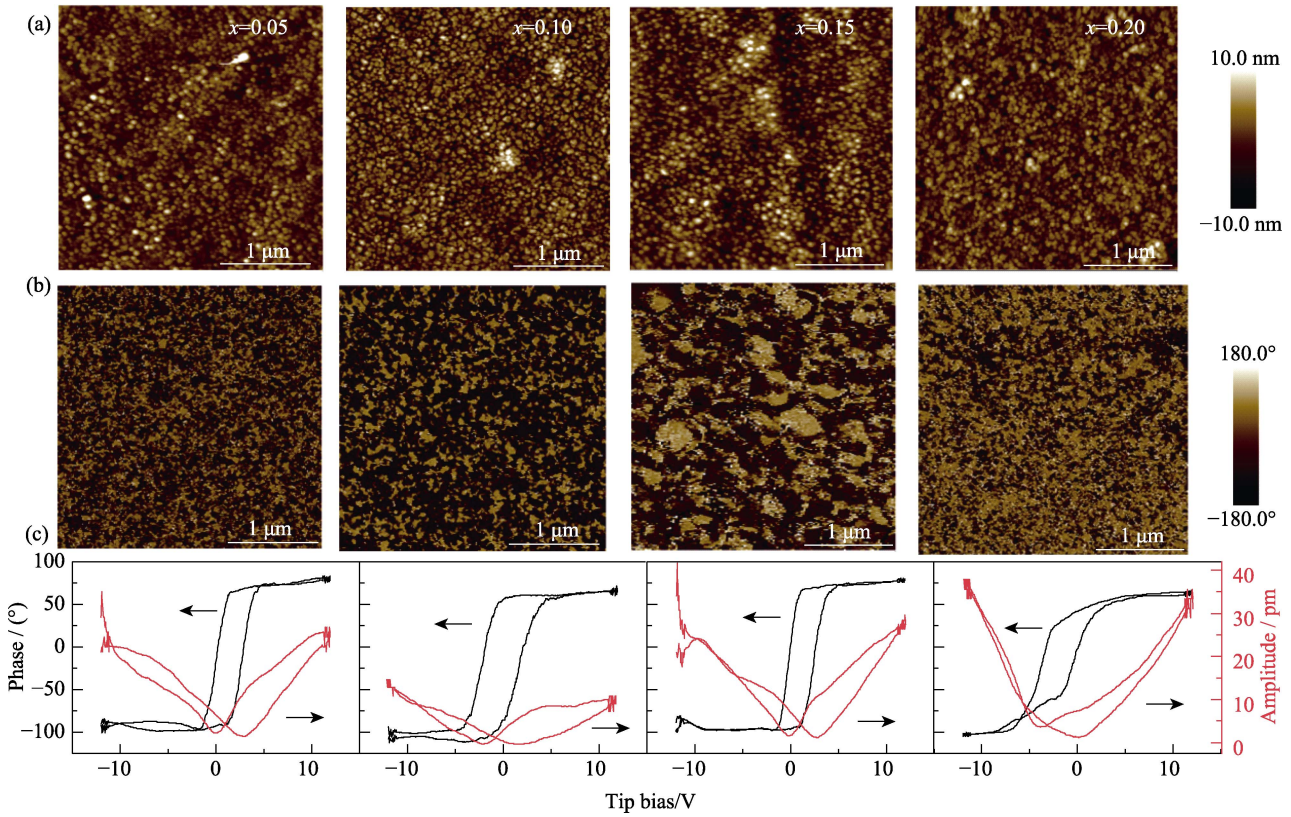

Fig. S1　AFM images, PFM images and asymmetric phase and amplitude loops *versus* tip bias voltage of BCFO (x=0.05, 0.10, 0.15, 0.20) films

Fig. S2 shows ferroelectric properties of BFO compositionally graded films. It is evident that with the increase in Ca doping concentration, the films progressively exhibit leakage characteristics, in contrast to the well-defined square-like and sharper *P-E* loops observed in BFO thin films. The variation trend of P_r and E_c of BCFO films with the increase of x are shown in the Fig. S2(f). The value of E_c increases gradually with the addition of Ca. It is commonly recognized that the E_c is primarily determined by the thin film's orientation, defects, thickness, and grain size. Here, the prevailing factor is believed to be defects, as the introduction of Ca^{2+} ions into the lattice results in the creation of oxygen vacancies to ensure electrical neutrality. And an increase in Ca doping concentration is expected to result in a corresponding rise in oxygen vacancies, causing an increase in E_c. However, the absence of a monotonic change in P_r with increasing x.

Narrow scan spectra of Bi4f of $Bi_{1-x}Ca_xFeO_3$ samples with x=0, 0.05, 0.10, 0.15 and 0.20 are shown in Fig. S3. The Bi4f doublet consists of two peaks at 158.5 and 163.8 eV, which are mainly identified as a signal from Bi-O bonds. The binding energy difference of the doublet peaks due to spin-orbit splitting is 5.3 eV, which is comparable to the theoretical value and their positions are in perfect agreement with those reported for Bi^{3+} in $BiFeO_3$. These observations confirm that Bi exists in its native oxidation state of Bi^{3+} in BCFO films.

Inverse piezoelectric coefficient of the thin film samples under an alternating current (AC) electric field

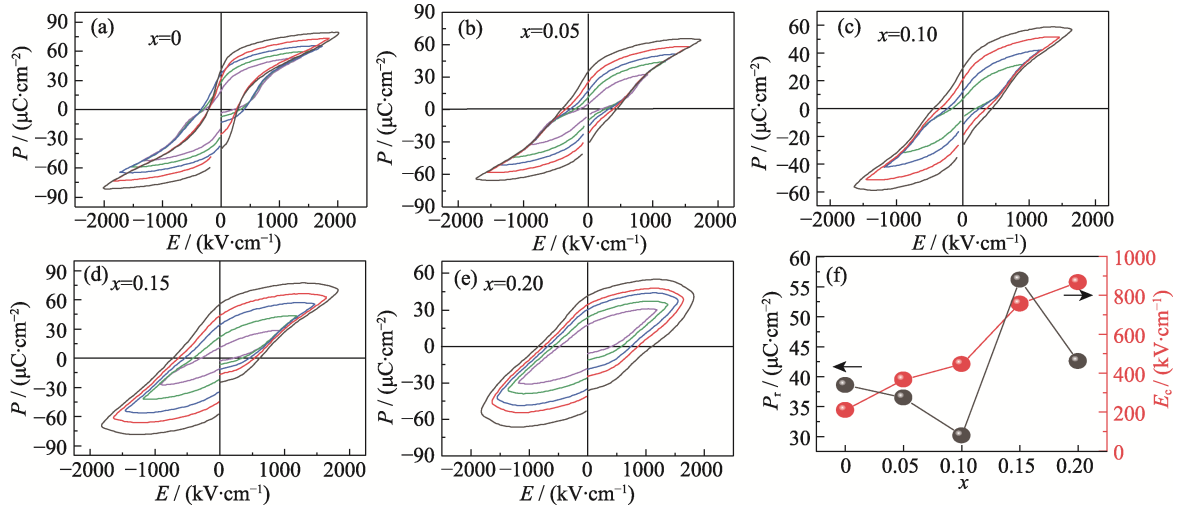

Fig. S2 Ferroelectric properties of $Bi_{1-x}Ca_xFeO_3$ films

(a) x=0; (b) x=0.05; (c) x=0.10; (d) x=0.15; (e) x=0.20; (f) The remanent polarization P_r, the coercive field E_c measured under the electric field intensity of 1800 kV·cm^{-1}

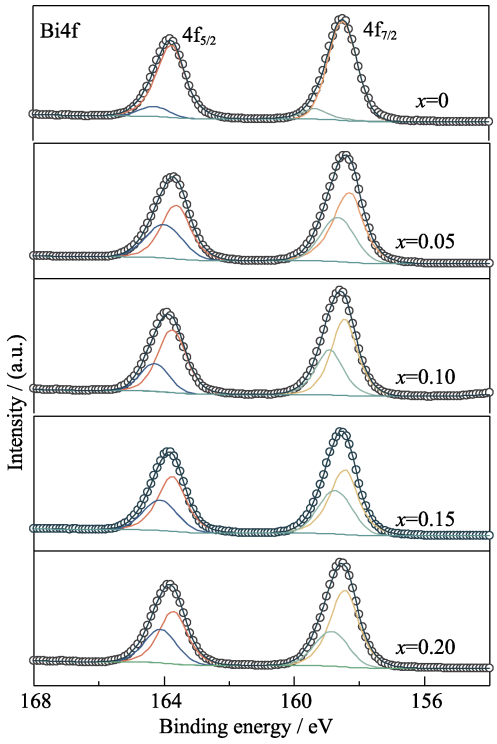

Fig. S3 Narrow scan spectra of Bi4f of $Bi_{1-x}Ca_xFeO_3$ samples with x=0, 0.05, 0.10, 0.15 and 0.20

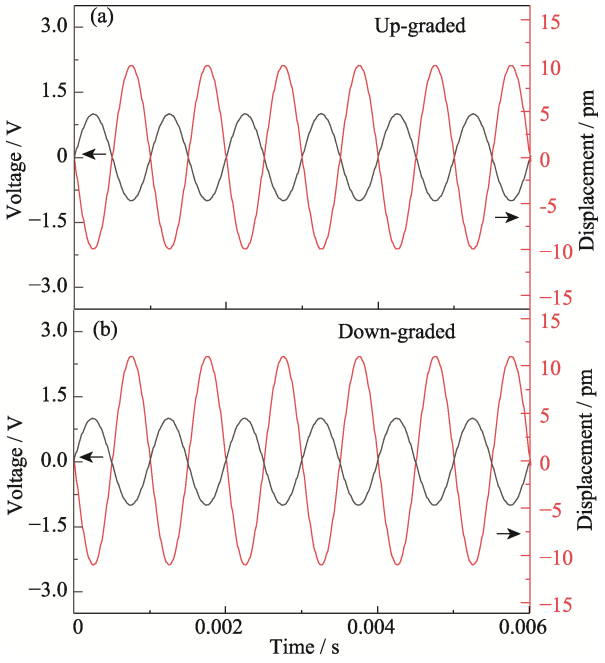

Fig. S4 Mechanical displacement of (a) up-graded BFO films and (b) down-graded BFO films as a function of time under an applied sinusoidal voltage

was measured using a doppler laser vibrometer (LDV, MSA-100-3D Micro System Analyzer, Polytec GmbH, Germany). Au electrodes with a diameter of 200 μm were sputtered on the films. Before measuring the electric-field-induced displacement, the substrate was clamped to a glass slide by using an adhesive. Both the smaller electrode and substrate clamping can reduce the substrate bending effect and mechanical resonances. A tungsten probe tip was contacted at the edge of the electrode whereas the substrate was grounded. During the measurement process, an alternating AC voltage of 1 V is applied to the top electrode, while the laser beam is directed to the center of the top electrode to measure both the magnitude and phase of the vibration. The measured mechanical displacement signals taken with doppler laser vibrometer as a response to the applied sinusoidal voltage of frequency 1 kHz and amplitude 1 V, as shown in Fig. S4. The inverse piezoelectric coefficient d_{33} is then simply calculated according to $d_{33} = \Delta t / V_{ac}$, where Δt is the amplitude of vibration of the thin films total pm. By simple calculation, d_{33} of the up-graded films and down-graded films are 10 pm/V and 11 pm/V, respectively. The self-polarization effect was confirmed by converse piezoelectric measurements.